Electrogenerated Chemiluminescence Biosensor for Detection of Mercury (II) ion via Target-Triggered Manipulation of DNA Three-Way Junctions

Fen Ma, Yu Chen, Yinchang Zhu, Jiawei Liu

www.elsevier.com/locate/talanta

PII: S0039-9140(18)31050-6
DOI: https://doi.org/10.1016/j.talanta.2018.10.004
Reference: TAL19120

To appear in: *Talanta*

Received date: 20 July 2018
Revised date: 28 September 2018
Accepted date: 7 October 2018

Cite this article as: Fen Ma, Yu Chen, Yinchang Zhu and Jiawei Liu, Electrogenerated Chemiluminescence Biosensor for Detection of Mercury (II) ion via Target-Triggered Manipulation of DNA Three-Way Junctions, *Talanta,* https://doi.org/10.1016/j.talanta.2018.10.004

Electrogenerated Chemiluminescence Biosensor for Detection of Mercury (II) ion via Target-Triggered Manipulation of DNA Three-Way Junctions

Fen Ma*, Yu Chen, Yinchang Zhu,Jiawei Liu*

Synthetic and Natural Functional Molecule Chemistry of Ministry of Education Key Laboratory, College of Chemistry and Materials Science, Northwest University, Xi'an, Shaanxi 710127, P. R. China

Abstract

A new electrogenerated chemiluminescence (ECL) biosensor is fabricated for the determination of mental ion incorporating DNA three-way junction structure (DNA-TWJ). As a model system, Hg^{2+} was chosen as an analyte. The ECL biosensor was fabricated by covalently coupling Hg^{2+} special DNA-TWJ tagged with ruthenium (II) complex (Ru) (named TW/Ru-J1) to the surface of glassy carbon electrode that had been covalently modified with 4-aminobenzoic acid via electrochemical oxidations. Upon binding of Hg^{2+} to the TW/Ru-J1, the confirmation of TW/Ru-J1 changed and induced Ru away from surface of electrode and thus led to a low ECL signal. The signal linearly decreases with the concentration of Hg^{2+} in the range from 0.1 pM to 10 pM with a detection limit of 0.04 pM. This study could be easily extended to various analytical platforms for the detection of many kinds of analytes or their interactions such as DNA/RNA, DNAzyme/target, aptamer/target, and antibody/antigen.

Keywords: Electrogenerated chemiluminescence; Biosensor, DNA three-way junction; Mercury (II) ion

1. Introduction

DNA has attracted great interest as a promising component of nanoscale architectures because of its well-ordered structures and highly programmable nature [1]. Of the various nucleic acid structures, DNA branching structures in general offer a unique window into DNA nanotechnology because more sophisticated structures can be assembled, as opposed to the sole use of one-dimensional DNA objects [2]. Among these DNA branching structures, DNA three-way junction (DNA-TWJ) is a unique branched structure and consists of three double helical arms connected at the junction point [3], [4]. Target-responsive DNA-TWJs can also be designed into DNA devices for molecular diagnostic, sensing, and imaging applications. One strategy of the target-responsive DNA-TWJ has involved attachment of a target-responsive domain as one of the three arms that form the junction, where conformational change in the domain upon binding to its target induces reorientation of the junction arms relative to one another [5]. In recent years, Wang group provided a DNA-TWJ-Based biosensing platform for detection of DNA, thrombin and ATP [6]. Le group developed binding-induced TWJ technique for prostate-specific antigen [5]. Wang and Liu

reported a catalytic hairpin assembly programmed DNA-TWJ strategy for the enzyme-free and amplified electrochemical detection of target DNA [7]. Ou yang group fabricated a label- and enzyme-free fluorescent sensor for the detection of single nucleotide polymorphisms [8]. Sen group and Yu group explored a series of unique DNA-TWJs biosensing principles [9], [10], [11], [12]. For example, Huang et al designed a new kind of DNA-TWJs for determination of thrombin [9]. The sensing principle of a new kind of DNA-TWJs is based on the incorporation of an anti-thrombin aptamer as the receptor, whose altered conformation upon thrombin binding switches on the conductivity of an adjacent helical conduction path, leading to an increase in the measured electrical signal through the sensor with a detection limit of 5 pM. Thomas et al reported the development of a made-to-order electronic sensor for determination of biomarker of lung cancer (CTAP III/NAP2) [11].

Hg^{2+} is one of the highly toxic environmental pollutants [13], [14] and microbial biomethylation of Hg^{2+} yields methyl mercury that could be accumulated in the body through the food chain and cause health problems such as brain damage and other chronic diseases [15]. Determination of Hg^{2+} can be achieved with a numbers of traditional analytical approaches, which include atomic absorption or emission spectroscopy [16] and selective cold vapor atomic fluorescence spectrometry [17]. These methods are sensitive but generally involve tedious sample preparation, expensive and sophisticated instrumentation which significantly limit their portability. It has been demonstrated that the Hg^{2+} can selectively bind between two DNA thymine (T) and form the stable T–Hg^{2+}–T pair [18]. Many alternative designs based on the highly specific interaction of Hg^{2+} with T for sensitive Hg^{2+} detection using, e.g., optical [19], [20], electrochemical [21], [22] and electrogenerated chemiluminescence biosensors [23], [24] were reported. We found that few works

designed biosensing devices to detect Hg^{2+} on basis of DNA-TWJ. For example, Ma group constructed a reversible molecular device in the nanoscale based on a DNA-TWJ fueled by Hg^{2+} [25]. Ju group designed a "signal-on" electrochemical sensing strategy for highly sensitive and selective detection of mercury (II) via its induction to DNA-TWJ [26]. The two DNA-TWJs molecular devices for Hg^{2+} were designed by the two groups based on hybridization of three ss-DNA, which possibly suffered non-specifically absorption and result in false positive signal.

Electrogenerated chemiluminescence (ECL) biosensors combine the advantages of both electrochemical and chemiluminescent biosensors, and are highly sensitive, easy to control and operate with inexpensive equipment, and exceedingly selective due to the use of the biological recognition elements in conjunction with specific ECL label and coreactant [27]. Up to now, few ECL biosensors were fabricated based on DNA-TWJs for molecular diagnostic, sensing, and imaging applications.

In this study, we first fabricated ECL biosensor on basis of DNA-TWJ for the determination of metal ion. Scheme 1 illustrated the working principle of the biosensor. The Hg^{2+} specific DNA-TWJ (named TW/Ru-J1 in this work) was constructed by 5′-amino-ss-DNA (TW) hybridazied with its complementary ss-DNA (J1) tagged with ruthenium complex at 5 terminal (Ru-J1), one arm of which is Hg^{2+}-binding domain containing thymine (T) bases. The ECL biosensor was fabricated by covalently coupling TW/Ru-J1 onto the surface of glass carbon electrode modified with 4-aminobenzoic acid. In the absence of Hg^{2+}, the biosensor adopts an open, unstacked conformation, which could allows efficient electron transfer from Ru complex to the electrode surface due to the tag close to the electrode surface and generate a strong ECL signal. And then, the binding of Hg^{2+} to T-T mismatches induces the adaptive folding and compaction of the TW/Ru-J1 because of

formation of T-Hg^{2+}-T base-pairs [18], resulting in a small the ECL signal due to the tag away from the electrode surface. The characteristics of the ECL biosensor and the analytical performance are investigated.

2. Experimental section

2.1. Reagents

4-aminobenzoic acid (4-ABA), N-(3-dimsethylaminopropyl)-N-ethyl carbodiimide hydrochloride (EDC) and N-hydrosuccinimide (NHS) were purchased from Sigma-Aldrich (USA). Tripropylamine and Tris (hydroxymethyl) amiomenthane were obtained from Shanghai Macklin Biochemical Co., Ltd (China). Mercury (Ⅱ) nitrate monohydrate was obtained from Sinopharm Chemical Reagent Co., Ltd (China). Magnesium chloride was obtained from Aladdin (China). Sodiun nitrite was obtained from Tianjin Shengao Chemical Reagent Co,. Ltd (China). All reagents were of analytical grade.

DNA-TWJ of TW/Ru-J1 containing the Hg^{2+}-specific thymine (T) bases were designed to be TW, 5′-amino-$(CH_2)_6$-O- TCT CCA GCG TCG TTT GTT TGC GGG AGC TTT CTT AAA TCT CGA GCT AAA-3', their complementary strand J1 (H_2N-$(CH_2)_6$-O-5'-TTT AGC TCG AGA CGA CGC TGG AGA-3'), the J1 was subjected to covalent coupling with Ru(bpy)$_2$(mcbpy-O-Su-ester)$(PF_6)_2$ (Ru) at 5 terminal and formed Ru-J1, all the sequences were designed according to the reference [12] and synthesized by Shanghai Sangon Biological Engineering Technology & Services Co., Ltd (China).

ECL measurements were done on MPI-E Ⅱ ECL detector (Xi'an Remax Analysis Instruments Co., Ltd (China), in which a photomultiplier tube (PMT) is biased on 900 V. A three-electrode system composed of a biosensor or a glass carbon electrode (GC ≈3mm) as working electrode, a platinum plate as counter electrode, and a Ag/AgCl

(saturated KCl) as reference electrode, was used. All potentials in this work were referred to the reference electrode.

2.2. Fabrication of ECL biosensor

2.0 μM of freshly prepared TW was hybridized with the 3.0 μM Ru-J1 in deoxygenated DNA immobilization buffer at 80 °C for 5 min to form the hybridized TW/Ru-J1, followed by slow cooling to room temperature in order to fold into the proper secondary structures. The electrochemical modification of 4-ABA on the surface of a clean GC was carried out in 0.5 M HCl solution containing 10mM 4-ABA and 8mM $NaNO_2$ by cyclic scanning between +0.5 and +2.0V for 4 cycles with a scan rate of $20mVs^{-1}$. The activation of the 4-ABA modified GC (4-ABA/GC) was performed by immersing 4-ABA/GC in 10mM tris-HCl buffer (pH 8.0) containing 5mM EDC and 8mM NHS for 0.5 h and then rinsed with 10mM tris-HCl buffer (pH 8.0). In second step, the ECL probe of TW/Ru-J1 was immobilized on the surface of the activated 4-ABA/GC. The activated electrode was immersed in prepared TW/Ru-J1 solution, allowing to stay for 1 h in a water-saturated atmosphere. The resulting electrode was thoroughly rinsed with DNA buffer. 30μL of 10mM tris-HCl (pH 8.0) buffer containing 1mM ethanolamine was dropped onto the surface of TW/Ru-J1, allowing to stay for 15 min to deactivate the remaining succinimide groups and to block unreacted active sites on the surface of the electrode. The obtained electrode was rinsed thoroughly with DNA buffer and then used as the ECL biosensor and stored in air at room temperature in the dark.

2.3. ECL measurement

The ECL biosensor fabricated was immersed in a solution containing 50mM tris-HCl buffer (pH 8.0) and a fixed concentration of Hg^{2+} for 30min in water bath of room temperature and then washed with DNA buffer. The ECL measurement was

performed using the ECL biosensor which had interacted with Hg^{2+} as working electrode at a constant potential of +1.20V in 3.0 mL of 50 mM tris-HCl buffer containing 50 mM TPA (pH 8.0).

3. Results and Discussions

3.1.Characteristics of the ECL biosensor

Fig. 1 shows the electrochemical impedance spectra of the electrodes in each step of the fabrication of the ECL biosensor. From Fig. 1, the electrochemical impedance spectra of the bare GC (line a) exhibits a very small semicircle domain, suggesting a very low electron-transfer resistance (R_{et}, 0.04 KΩ). When the 4-ABA was electrochemically modified on the GC (line b), the R_{et} increased from 0.04 KΩ to 3.93 KΩ. Electrochemical modification of 4-ABA on GC electrode generates 4-ABA layer covered on the GC surface. And the surface coverage could be estimated from integration of the charge passed under the oxidation peak on the first scan (as shown in Fig. S1, See supporting information), reach 3.80×10^{-8} mol/cm^2 [28]. The carboxyl group of the 4-ABA will be deprotonated when EIS measurements were performed in 50 mM tris-HCl buffer (pH 8.0) containing 10 mM $Fe(CN)_6^{3-/4-}$ and 1 M KCl, since the pH 8.0 of tris-HCl buffer is higher than the acidity coefficient (pK_a) of 4.21 inferred from benzoic acid when 4-ABA covalently modified on glassy carbon electrode. Therefore, it can be deduced that 4-ABA modified on the GC surface blocks the electrode surface and the full deprotonation of carboxyl group of the 4-ABA makes an electrostatic repulsive force to $[Fe(CN)_6]^{3-/4-}$ [29]. As the TW/Ru-J1 designed was covalently coupled to carboxyl group of the 4-ABA (line c), the R_{et} decreased from 3.93 KΩ to 2.77 KΩ. This is attributed to two facts. Firstly, 4-ABA possibly desorbed from the surface of GC. The other one is $[Fe(CN)_6]^{3-/4-}$ was wrapped in the layer of 4-ABA on the surface of GC. After ethanolamine was dropped

onto the surface of TW/Ru-J1 modified electrode to (line d), the R_{et} increased from 2.77 KΩ to 3.41 KΩ. This indicates that the ethanolamine deactivate the remaining succinimide groups and to block unreacted active sites on the surface of the electrode. The biosensor was also characterized by cyclic voltammetry (CV) (as shown in Fig. S2 in supporting information), confirming that the biosensor was successfully fabricated.

Fig. 2 shows ECL kinetic profiles of the ECL biosensor before (line a) and after interaction with 0.1 pM Hg^{2+} (line b) and 0.5 pM Hg^{2+} (line c). Compared line a with line b, the ECL biosensor with interaction of 0.1 pM Hg^{2+} displayed a decreased signal. This indicates that the ECL biosensor has a response to analyte Hg^{2+}. Compared line b with line c, it can be clearly observed that the ECL intensity continued to decrease from 810 to 208 as the Hg^{2+} concentration is elevated. From the result, it can be deduced that the ECL biosensor displays signal off trend with increasing Hg^{2+} concentration. Prior study on DNA switch reported by Thomas et al have studyed the changed conformation of the Hg^{2+}-specific DNA-TWJ based on footprinting analysis and FRET measurements [12]. They found that Hg^{2+} addition leads to decreased acceptor emission and increased donor emission, which indicates decreased FRET energy transfer due to increased separation of the fluorophores. And they calculated change in the average angle between the stems of DNA-TWJs from ~101° to ~143° upon Hg^{2+} binding. The TW/Ru-J1 used in our work was derived from Thomas's study. Therefore, the possible reason of the signal off ECL biosensor designed in our work is that Hg^{2+} binding to TW/Ru-J1 resulted in the conformation of TW/Ru-J1 on the surface of electrode and made the Ru tag away from the electrode surface. In conclusion, the ECL sensor fabricated can be used to detect Hg^{2+} because changed concentrations of Hg^{2+} induced changed ECL signals.

3.2.Optimization of test conditions

The surface coverage of the ECL probe on 4-ABA/GC is expected to affect the ECL intensity of the biosensor towards Hg^{2+} detection, because a low surface coverage corresponds to a limited number of Ru complexes available for ECL generation, whereas a highly condensed surface coverage could sterically hinder the conformation change of the TW/Ru-J1 structure. Since the concentration of TW employed during DNA biosensor fabrication directly influence the surface coverage of the ECL probe on 4-ABA/GC, the concentration of TW for fabrication of the biosensor is optimized. The dependence of the ECL intensity of the biosensor on the concentration of the TW was investigated. The maximum ΔI_{ECL} was occurred at the concentration of 2.0 μM TW after interaction of Hg^{2+}, which was consistent with our earlier prediction. That was, the obtained surface coverage of the ECL probe on 4-ABA/GC surface was high enough but not crowded under present experimental conditions. Therefore, the concentration of 2.0 μM TW was used in the following experiments.

To maximize the ECL performance of the biosensor for Hg^{2+} detection, the applied potential of the biosensor with Hg^{2+} was examined. The ECL intensity of the Hg^{2+} bound biosensor is a function of the potential, in which a peak ECL is located at the applied potential of 1.20 V (Fig. 3). With the further increase of the applied potential, however, ΔI_{ECL} decreases. This could be related to the oxidation of water that produces extra amounts of oxygen, resulting in the consumption of $TPrA^{\bullet}$ free radicals needed for the generation of the excited state Ru1* species [24].

3.3.Performance of ECL biosensors

Fig. 4 shows the ECL profiles of the ECL biosensors after interaction with different concentrations of Hg^{2+} under the optimized conditions. From inset of Fig. 4,

it can be seen that ECL intensity decreased with an increase of the concentration of Hg^{2+} in the range from 0.1 pM to 10 pM. The linear regression equation was S = -1523.4 C + 920.2 (S is the ECL intensity, unit of C is pM) with a correlation coefficient value (R^2) of 0.981. The obtained detection limit of 0.04 pM is much lower than that from other latest reported methods based on T–Hg^{2+}–T interactions as shown in Table 1, which includes fluorescent probes based on evanescent wave fluorescence excitation [19], electrochemical biosensors [22], and Fluorescence biosensors [30], electrochemiluminescence biosensors [31]. The lower detection limit obtained in this work is attributed to the fact that the Hg^{2+} manipulation of DNA-TWJ of TW/Ru-J1 and the C–N covalently coupling method are used for the design of the ECL biosensor. This greatly benefits super-trace analysis of Hg^{2+}.

The selectivity of the biosensor was evaluated by challenging it with several metal ions. The ECL intensity of the biosensor fabricated was measured after it was interacted with each cation individually. The result is showed in Fig. 5. From Fig. 5, it can be seen that the changed ECL intensity of the biosensor with interaction of Cu^{2+}, or Zn^{2+}, Pb^{2+}, Mn^{2+}, Ca^{2+}, Fe^{3+} in the concentration of 10 pM is nearly same as that in the absence of Hg^{2+} (blank) and is much lower than that with interaction of 1 pM Hg^{2+}. Additionally, the ECL responses from 20 nM of the above common co-existing metal ions (Cu^{2+}, or Zn^{2+}, Pb^{2+}, Mn^{2+}, Ca^{2+}, Fe^{3+}) were in the similar range of the blank. And the changed ECL intensities are less than 8% of that from 1 pM Hg^{2+}. This indicates that the ECL biosensor has a good selectivity for discriminating Hg^{2+} from other metal ions tested.

Fig. 6 shows the ECL response of the ECL biosensor fabricated after interaction with 0.7 pM Hg^{2+} at a constant potential of +1.20 V for 12 cycles. The relative standard deviation of the ECL intensity of the ECL biosensor for 12 cycles was 5.0%.

The result indicates that the ECL biosensor fabricated using C-N covalently coupling method in this work showed a good stability.

The application of the ECL biosensor was evaluated via the determination of Hg^{2+} in water samples collected from three water pipes (Northwest University, China). As listed in Table 2, the results determined by the ECL biosensor are in good agreement with those obtained from the cold vapor atomic fluorescence spectrometry (CVAFS) method. The relative deviations were 7.7 %, 6.0% and 3.1 %, which were obtained by dividing the difference between the results obtained using the CVAFS method and the ECL biosensor by the values obtained using the CVAFS method. F test and t test were used to evaluate the application of ECL biosensor. As shown in Table 2, all the calculated values of F and t calculated are smaller than the values of standard F and t (95% of confidence level), which indicated that there is no significant difference between the ECL biosensor and CVAFS method. The results demonstrated that the designed ECL biosensor can be used to real samples determination.

4. Conclusion

A novel ECL biosensor for highly sensitive determination of Hg^{2+} has been developed on the basis of the DNA-TWJs of TW/Ru-J1 as an ECL probe. The ECL biosensor fabricated has the lowest detection limit of Hg^{2+} (0.04 pM) so far, good stability and selectivity. The strategy can open a new door toward the development of the detection method for metal ions or biomarkers on biochips.

Acknowledgement

We would like to thank National Natural Science Foundation of China (No. 21605120), the Natural Science Foundation of Shaanxi Province (2018JQ2010) and the Fundamental Research Fund of Northwest University (15NW11).

References

[1] J. L. Duprey, Y. Takezawa, Metal-locked DNA three-way junction, Angew. Chem. Int. Ed. 125 (2013) 1250-1254.

[2] I. T. Seemann, V. Singh, M. Azarkh, M. Drescher, J. S. Hartig, Small-molecule-triggered manipulation of DNA three-way junctions, J. Am. Chem. Soc. 133 (2011) 4706-4709.

[3] Y. C. Huang, A. K. Cheng, H. Z. Yu, D. Sen, Charge conduction properties of a parallel-stranded DNA G-quadruplex: implications for chromosomal oxidative damage, Biochemistry 48 (2009) 6794-6804.

[4] R. P. Fahlman, D. Sen, DNA conformational switches as sensitive electronic sensors of analytes, J. Am. Chem. Soc. 124 (2002) 4610-4616.

[5] F. Li, Y. Lin, X. C. Le, Binding-induced formation of DNA three-way junctions and its application to protein detection and DNA strand displacement, Anal. Chem. 85 (2013) 10835-10841.

[6] L. B. Zhang, S. J. Guo, J. B. Zhu, Z. X. Zhou, T. Li, J. Li, S. J. Dong, E.Wang, Engineering DNA three-way junction with multifunctional moieties: sensing platform for bioanalysis, Anal. Chem. 87 (2015) 11295-11300.

[7] S. Liu, W. Wei, T. Liu, L. Wang, Catalytic hairpin assembly-programmed DNA three-way junction for enzyme-free and amplified electrochemical detection of target DNA, Chem. Asian. J. 10 (2015) 1903-1908.

[8] F. Sun, Y. You, J. Liu, Q. Song, X. Shen, N. Na, J. Ouyang, DNA three-way junction for differentiation of single-nucleotide polymorphisms with fluorescent

copper nanoparticles, Chemistry 23 (2017) 6979-6982.

[9] Y. C. Huang, B. Ge, D. Sen, H. Z. Yu, Immobilized DNA switches as electronic sensors for picomolar detection of plasma proteins, J. Am. Chem. Soc. 130 (2008) 8023-8029.

[10] J. M. Thomas, H. Z. Yu, D. Sen, DNA electronic switches based on analyte-responsive aptamers, Methods. Mol. Biol, 1103 (2014) 267-276.

[11] J. M. Thomas, B. Chakraborty, D. Sen, H. Z. Yu, Analyte-driven switching of DNA charge transport: de novo creation of electronic sensors for an early lung cancer biomarker, J. Am. Chem. Soc. 134 (2012) 13823-13833.

[12] J. M. Thomas, H. Z. Yu, D. Sen, A mechano-electronic DNA switch, J. Am. Chem. Soc. 134 (2012) 13738-13748.

[13] K. M. Rice, E. M. Walker, M. Wu, C. Gillette, E. R. Blough, Environmental mercury and its toxic effects, J. Prev. Med. Public. Health. 47 (2014) 74-83.

[14] L. Magos, T. W. Clarkson, Overview of the clinical toxicity of mercury, Ann. Clin. Biochem. 43 (2006) 257-268.

[15] E. M. Nolan, S. J. Lippard, Tools and tactics for the optical detection of mercuric ion, Chem. Rev. 108 (2008) 3443-3480.

[16] I. L. S. Almeida, M. D. R. Oliveira, J. B. B. Silva, N. M. M. Coelho, Suitable extraction of soils and sediments for mercury species and determination combined with the cold vapor generation atomic absorption spectrometry technique, Microchem. J. 124 (2016) 326-330.

[17] L. N. Liang, G. B. Jiang , J. F. Liu and J. T. Hu , Speciation analysis of mercury

in seafood by using high-performance liquid chromatography on-line coupled with cold-vapor atomic fluorescence spectrometry via a post column microwave digestion, Anal. Chim. Acta. 477 (2003) 131-137.

[18] Y. Miyake, H. Togashi, M. Tashiro, H. Yamaguchi, S. Oda, M. Kudo, Y. Tanaka, Y. Kondo, R. Sawa, T. Fujimoto, T. Machinami, A. Ono, MercuryII-mediated formation of thymine-Hg (II)-thymine base pairs in DNA duplexes, J. Am. Chem. Soc. 128 (2006) 2172-2173.

[19] R.Wang, X. Zhou, H. Shi, Y. Luo, T–T mismatch-driven biosensor using triple functional DNA-protein conjugates for facile detection of Hg^{2+}, Biosens. Bioelectron. 78 (2016) 418-422.

[20] A. Ono, H. Togashi, Highly selective oligonucleotide-based sensor for mercury (II) in aqueous solutions, Angew. Chem. Int. Ed. 43 (2004) 4300-4302.

[21] M. Q. Hong, M. Y. Wang, J. Wang, X. Q. Xu, Z. Y. Lin, Ultrasensitive and selective electrochemical biosensor for detection of mercury (II) ions by nicking endonuclease-assisted target recycling and hybridization chain reaction signal amplification, Biosens. Bioelectron. 94 (2017) 19-23.

[22] A. Xu, L. Chao, H. Xiao, Y. Sui, J. Liu, Q. Xie and S. Yao, Ultrasensitive electrochemical sensing of Hg^{2+} based on thymine-Hg^{2+}-thymine interaction and signal amplification of alkaline phosphatase catalyzed silver deposition, Biosens. Bioelectron. 104 (2018) 95-101.

[23] J. Li, L. P. Lu, T. F. Kang, S. Y. Cheng, Intense charge transfer surface based on graphene and thymine-Hg (II)-thymine base pairs for detection of Hg^{2+}, Biosens.

Bioelectron. 77 (2016) 740-745.

[24] F. Ma, Y. Zhang, H. L. Qi, Q. Gao, C. X. Zhang, W. J. Miao, Ultrasensitive electrogenerated chemiluminescence biosensor for the determination of mercury ion incorporating G4 PAMAM dendrimer and Hg (II)-specific oligonucleotide Biosens. Bioelectron. 32 (2012) 37-42.

[25] L. Ma, G. Wu, Y. Li, P. Qin, L. Meng, H. Liu, Y. Li, A. Diao, A reversible metal ion fueled DNA three-way junction molecular device for "turn-on and -off" fluorescence detection of mercury ions (II) and biothiols respectively with high selectivity and sensitivity, Nanoscale 7 (2015) 18044-18048.

[26] L. Cui, J. Wu, M. Li, H. X. Ju, Highly sensitive electrochemical detection of mercury (II) via single ion-induced three-way junction of DNA, Electrochem. Commun. 59 (2015) 77-80.

[27] W. Miao, Electrogenerated Chemiluminescence and Its Biorelated Applications, Chem. Rev. 108 (2108) 2506-2553.

[28] S. S. Yu, E. S. Tan, R. T. Jane, A. J. Downard, An electrochemical and XPS study of reduction of nitrophenyl films covalently grafted to planar carbon surfaces, Langmuir 23 (2007) 11074-11082.

[29] J. Liu, C. Long, B. f. Liu, S. J. Dong, Covalent modification of a glassy carbon surface by 4-Aminobenzoic Acid and its application in fabrication of a polyoxometalates-consisting monolayer and multilayer films, Langmuir 16 (2000) 7471-7476.

[30] X. Li, J. Xie, B. Jiang, Metallo-toehold-activated catalytic hairpin assembly formation of three-way DNAzyme junctions for amplified fluorescent detection

of Hg^{2+}, ACS Appl. Mater. Interfaces. 9 (7) 2017 5733-5738.

[31] X. Y. Jiang, H. J. Wang, H. J. Wang, R. Yuan and Y. Q. Chai, Signal-switchable electrochemiluminescence system coupled with target recycling amplification strategy for sensitive mercury ion and mucin 1 assay, Anal. Chem. 8 (18) 2016 9243-9250.

Figures and Captions

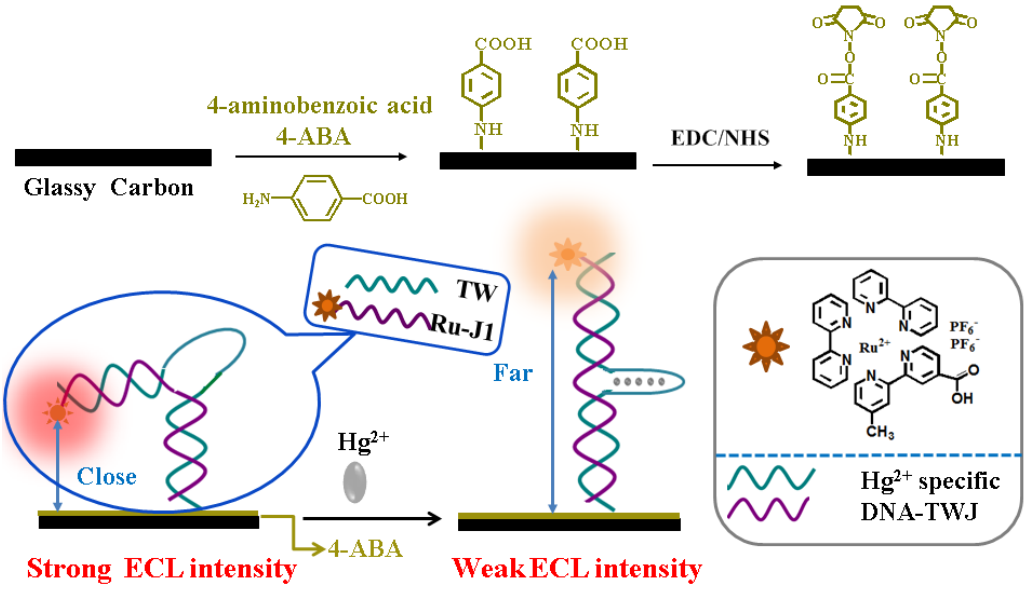

Scheme 1 Schematic diagram of the fabrication of DNA-TWJ-based ECL biosensor for the detection of Hg^{2+}.

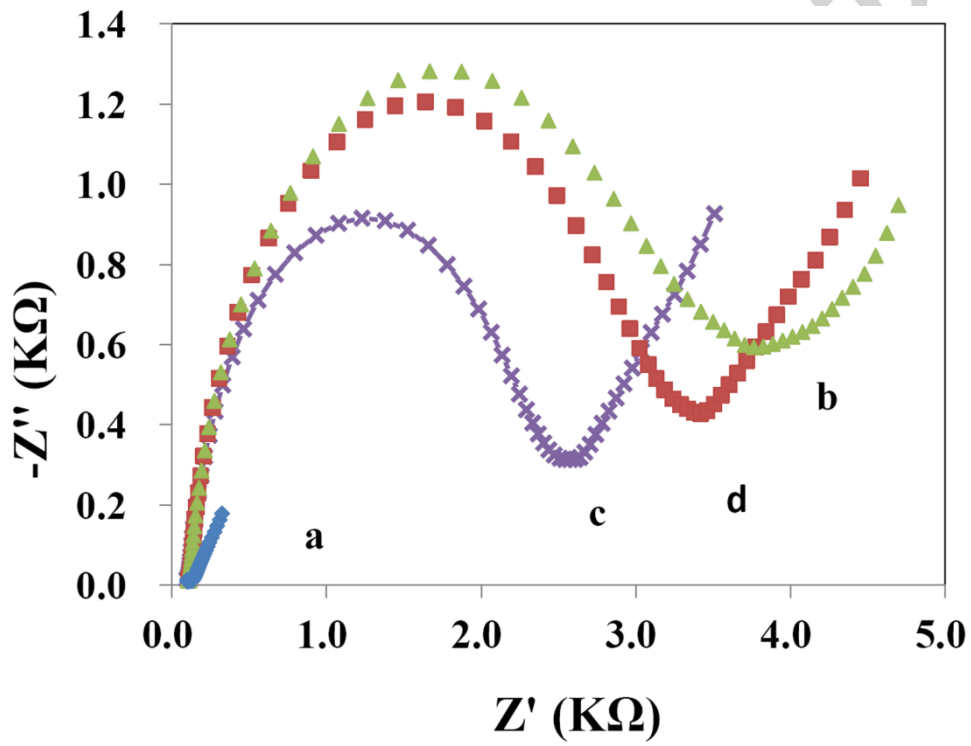

Fig. 1 Electrochemical impedance spectra of the electrodes in each step of the fabrication of the ECL biosensor. (a) Bare GC; (b) 4-ABA/GC; (c) TW/Ru-J1/4-ABA/GC; (d) ethanolamine/ TW/Ru-J1/4-ABA/GC. All measurements were performed in 5 mM $K_3Fe(CN)_6$–5 mM $K_4Fe(CN)_6$–50 mM tris-HCl–0.1M KCl (pH 8.0). Bias potential, 0.232 V; frequency, 100 kHz to 1.0 Hz; amplitude, 5.0 mV.

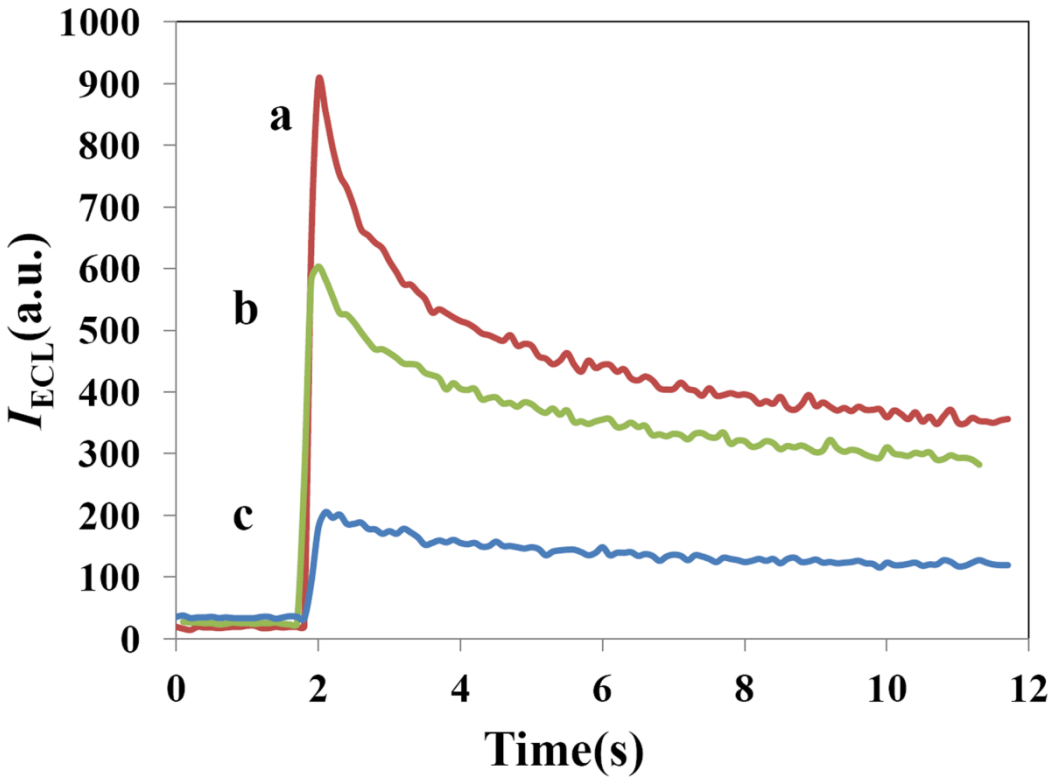

Fig. 2 ECL responses of ECL biosensors at +1.2V in 50 mM tris-Hcl buffer (pH 8.0) containing 50 mM TPA (a) without interaction of Hg^{2+}, (b) with interaction of 0.1 pM Hg^{2+}, (c) with interaction of 0.5 pM Hg^{2+}.

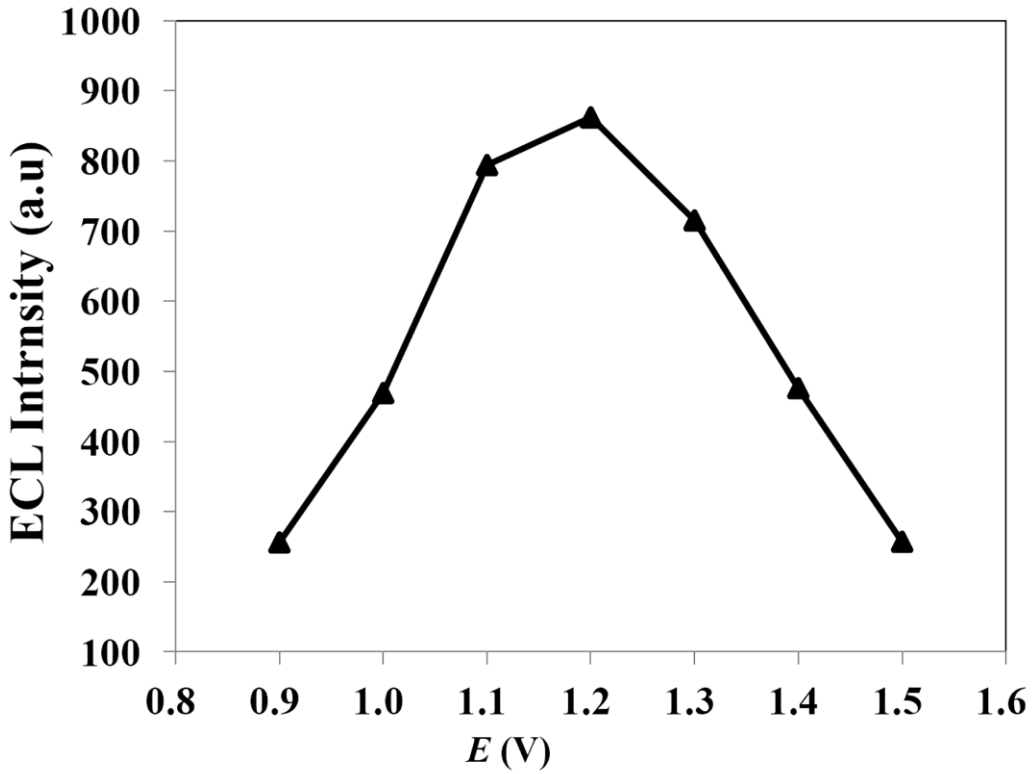

Fig. 3 Dependence of the changed ECL peak intensity (ΔI) of the ECL biosensor on applied potential after the interaction with 1pM Hg^{2+}, obtained in 50mM Tris-HCl buffer (pH 8.0) containing 50mM TPA. $\Delta I = I_0 – I$, where I_0 and I were the ECL peak intensity before and after the ECL biosensor was interacted with Hg^{2+}, respectively.

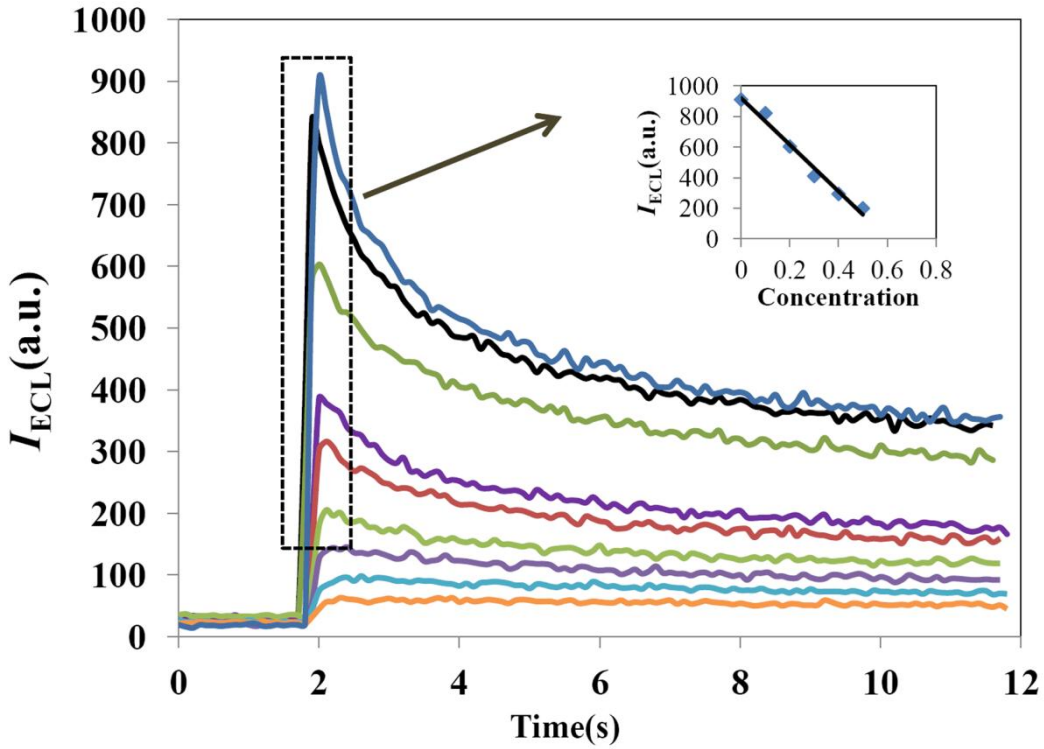

Fig. 4 ECL responses of the ECL biosensors with interaction of Hg^{2+} in different concentrations. 0 pM, 0.1 pM, 0.2 pM, 0.3 pM, 0.4 pM, 0.5 pM, 0.7 pM, 1 pM, 3 pM, 10 pM. The ECL measurement condition is same as Figure 1.

Table 1. Comparison between the biosensor in the work and latest reported methods

Method	Detection range	Detection limit	References
Evanescent wave fluorescence excitation	75 nM to 1 mM	1.06 nM	19
Fluorescence	10 pM to 100 nM	4.5 pM	30
Electrochemical	2.5 mM to 1 mM	0.5 mM	22
Electrochemiluminescence	10 pM to 100 nM	3.1 pM	31
Electrochemiluminescence	0.1pM to 10 pM	0.04 pM	this work

Table 2. Determination of Hg^{2+} in water samples using the ECL biosensor and the CVAFS method.[a]

Water sample	ECL biosensor	CVAFS[a]	F test		t test	
	detected (pM) n=3	detected (pM) n=3	$F_{calculated}$	[b]F	$t_{calculated}$	[b]t
Water pipe 1	0.48±0.07	0.52±0.07	1.00		0.70	
Water pipe 2	0.47±0.03	0.50±0.03	1.00	19.00	1.22	2.13
Water pipe 3	0.53±0.03	0.58±0.03	1.00		2.04	

[a] All values were obtained as an average of three repetitive measurements plus the standard deviation. [b]confidence level is 95%.

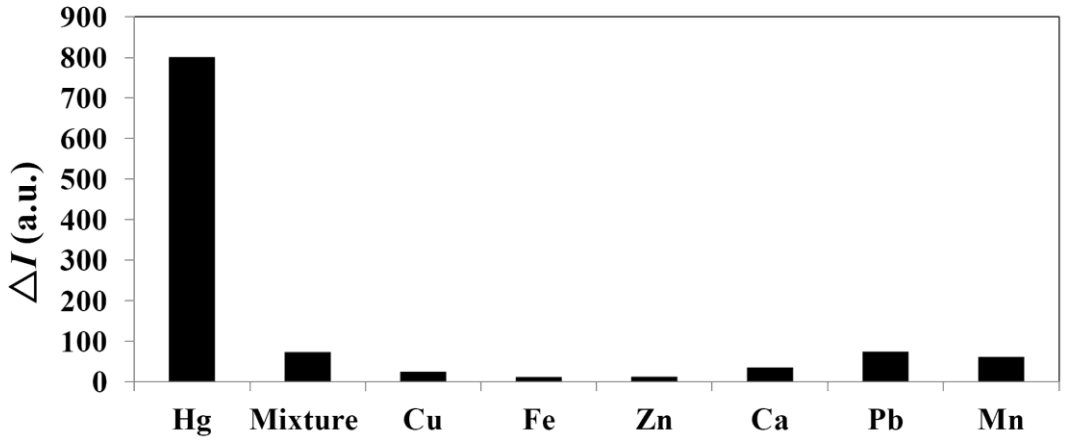

Fig. 5 The changed ECL intensity ($\triangle I$) of the ECL biosensors after individual interaction with 1 pM Hg^{2+} or 10 pM metal ion (Cu^{2+}, Zn^{2+}, Mn^{2+}, Co^{2+}, Ca^{2+}, Fe^{3+}) or 20 nM of mixture metal ions (Cu^{2+}, Zn^{2+}, Mn^{2+}, Co^{2+}, Ca^{2+}, Fe^{3+}). The ECL measurement condition is same as Fig. 1. $\triangle I = I_0 – I$, where I_0 and I were the ECL peak intensity before and after the ECL biosensor was interacted with Hg^{2+}, respectively.

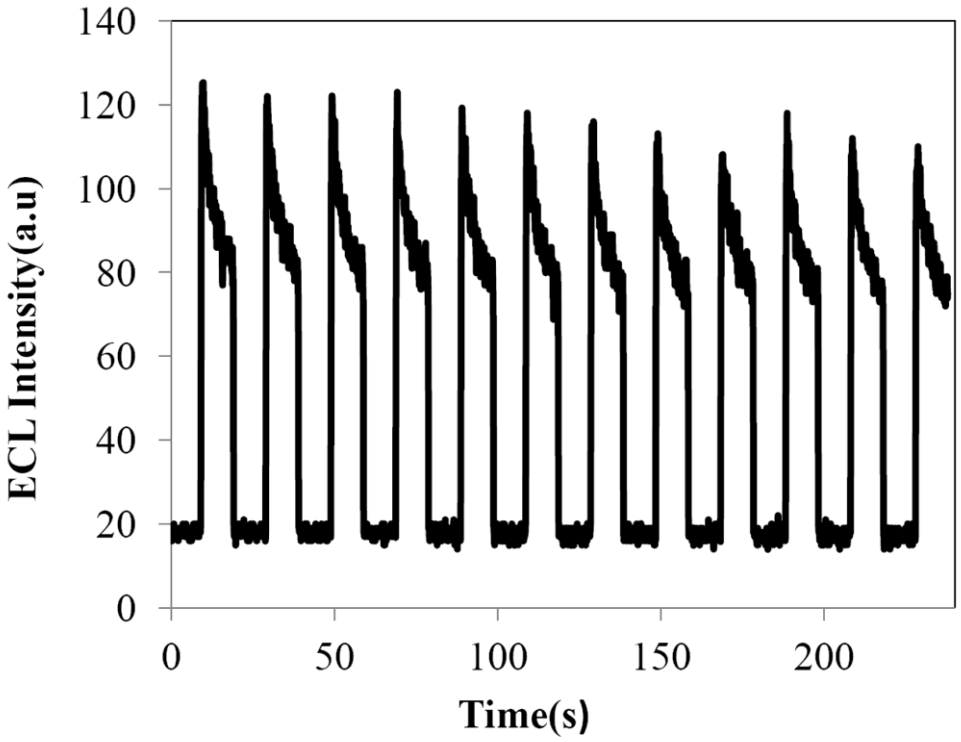

Fig. 6 ECL continual response of the ECL biosensor obtained at +1.2 V in 50 mM TPA-50 mM tris-HCl buffer (pH 8.0) after the sensor was interacted with 0.7 pM Hg^{2+}.

Highlights

- DNA three-way junction (DNA-TWJ) is a unique branched structure and consists of three double helical arms connected at the junction point.
- Electrogenerated chemiluminescence (ECL) biosensors combine the advantages of both electrochemical and chemiluminescent biosensors, and are highly sensitive, easy to control and operate with inexpensive equipment, and exceedingly selective.
- First designed ECL biosensor on basis of DNA-TWJ for the determination of mercury ion is fabricated.
- The obtained detection limit of 0.04 pM is much lower than that from other latest reported methods based on T–Hg^{2+}–T interactions.
- The strategy can open a new door toward the development of the detection method for metal ions or biomarkers on biochips.